

Supercurrent-induced Skyrmion dynamics and Tunable Weyl points in Chiral Magnet with Superconductivity

Rina Takashima¹ and Satoshi Fujimoto²

¹*Department of Physics, Kyoto University, Kyoto 606-8502, Japan and*

²*Department of Materials Engineering Science, Osaka University, Toyonaka 560-8531, Japan*

(Dated: March 11, 2022)

Recent studies show superconductivity provides new perspectives on spintronics. We study a heterostructure composed of an *s*-wave superconductor and a cubic chiral-magnet that can stabilize a topological spin texture, a skyrmion. We propose a supercurrent-induced spin torque that originates from the spin-orbit coupling, and we show that the spin torque can drive a skyrmion in an efficient way that reduces Joule heating. We also study the band structure of Bogoliubov quasiparticles and show the existence of Weyl points, whose positions can be controlled by the direction of the magnetization. This results in an effective magnetic field acting on the quasiparticles in the presence spin textures. Furthermore, the tilt of the Weyl cones can also be tuned by the strength of the spin-orbit coupling, and we propose a possible realization of type-II Weyl points.

PACS numbers:

I. INTRODUCTION

Topological structures in states of matter exhibit interesting features more than just the topological stability. Topological insulators have surface Dirac cones, and show the magnetoelectric polarizability[1, 2]. Weyl points in a band structure are predicted to produce a variety of phenomena such as Fermi-arc surface states, chiral anomaly, and unusual anomalous Hall effects [3–15]. In a spin texture, of particular recent interest is a magnetic skyrmion[16–21], which is defined by an integer topological number. Skyrmions are experimentally observed in some chiral magnets such as cubic B20 compounds MnSi and Fe_{0.5}Co_{0.5}Si. Their topological structure gives rise to Magnus force that acts on a skyrmion like a Lorentz force[22]. When electrons coupled to skyrmions, the so-called emergent electromagnetic field acts on electrons [21, 23].

Skyrmions have received attentions also as a promising candidate of a future information career. Magnus force prevents a skyrmion from being pinned by impurities or lattice defects, and the threshold current density to drive its motion is quite low compared to that of a domainwall [24–29]. Such current-induced magnetization dynamics has been studied intensively in the field of spintronics. A spin transfer torque[30–33] is one of current-induced spin torque, which occurs in the presence of noncollinear spin textures. Spin-orbit (SO) coupling realizes another type of current-induced torque, so called SO torque[34–38], which can also drive domain walls[39] or skyrmions via applied currents[40, 41].

Recently, more and more studies show that superconductivity provide new perspectives on spintronics[42–62]. For application, supercurrents may realize efficient ways to control magnetization that minimizes Joule heating, which can be a critical issue when one controls magnetic dynamics by an applied current. From a theoretical point of view, systems with superconductivity and magnetization are also interesting in the band topology of Bogoliubov quasiparticles. With Rashba SO coupling[63–67] or spin textures[68–71], bands of quasi particle have nontrivial topology; topological superconductors can be realized. It would also be an important issue to

utilize the realized topological transport phenomena for spin dynamics, and systems with superconductivity and magnetization are promising platforms for novel spintronics application.

In this paper, we study supercurrent-induced skyrmion dynamics in a heterostructure composed of an *s*-wave superconductor and a cubic chiral magnet (e.g. MnSi and Fe_{0.5}Co_{0.5}Si). To this end we consider SO coupling in chiral magnets which can be written as $H_{so} = \alpha_{so} \mathbf{k} \cdot \boldsymbol{\sigma}$, around Γ point with $\boldsymbol{\sigma}$ being the pauli matrices acting on spin space. This SO coupling plays a crucial role in chiral magnets, since it leads to Dzyaloshinskii-Moriya interaction, which is the origin of the noncollinear magnetic orders such as helical spin orders and skyrmion crystal phases. With the SO coupling, we calculate a spin polarization and a resulting spin-torque induced by *supercurrents* instead of resistive currents to manipulate skyrmions.

Another aim of this paper is to study the topological structure in the Bogoliubov quasiparticle band in the heterostructure. We show that the band has a pair of Weyl points, and the positions of them can be controlled by the direction of magnetization. Consequently, inhomogeneous spin textures realize an effective magnetic field acting on Bogoliubov quasiparticles. Furthermore, the tilt of the Weyl cones can also be tuned by the strength of the SO coupling. Recently, *type-II* Weyl points, whose dispersion is strongly tilted so that it has a finite density of states at each Weyl point, are proposed in materials such as LaAlGe[72], MoTe₂[73–76], and WTe₂[77–79]. They are predicted to have peculiar properties[80–82]; chiral anomaly depending on the relative direction of the field and tilt[83], and a non-analytic behavior in the anomalous hall effect[84]. For our superconducting system, we propose a realization of type-II Weyl points in a quasiparticle spectrum, and we show a transition between conventional (type-I) Weyl points and type-II Weyl points. Combined with the effective magnetic field due to the spin texture, we expect intriguing transport properties to be realized in our system.

The organization of this paper is as follows. In Sec. II, we introduce a model, which describes a cubic chiral magnet with proximity induced superconductivity. In Sec. III, using a lin-

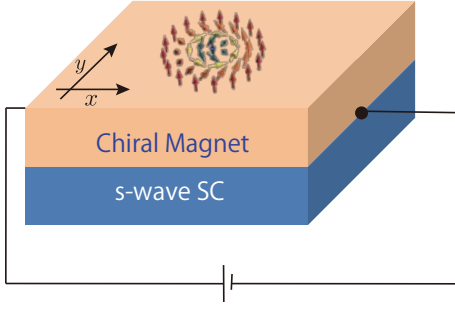


FIG. 1: Heterostructure composed of a chiral magnet and an s -wave superconductor.

ear response theory, we calculate spin polarization induced by a supercurrent, which acts as a local spin torque that drives motions of skyrmions. In Sec. IV, we study the band structure of Bogoliubov quasiparticles, and demonstrate how type-I (conventional) and type-II Weyl points appear. We also discuss the effect of inhomogeneity in spin textures. Sec. V is devoted to the summary and discussions.

II. MODEL

We consider a heterostructure composed of an s -wave superconductor and a cubic chiral magnet (Fig. 1), which is modeled by the following Hamiltonian:

$$\mathcal{H} = \frac{1}{2} \sum_{\mathbf{k}} (c_{\mathbf{k}\uparrow}^\dagger, c_{-\mathbf{k}\downarrow}^\dagger) H(\mathbf{k}) \begin{pmatrix} c_{\mathbf{k}} \\ (c_{-\mathbf{k}}^\dagger)^T \end{pmatrix}, \quad (1)$$

where $c_{\mathbf{k}}^T = (c_{\mathbf{k}\uparrow}, c_{\mathbf{k}\downarrow})$ are annihilation operators for electrons of spin up and down. The Bogoliubov de Gennes (BdG) Hamiltonian $H(\mathbf{k})$ is

$$H(\mathbf{k}) = \begin{pmatrix} H_0(\mathbf{k}) & i\Delta\sigma_y \\ -i\Delta^*\sigma_y & -H_0(-\mathbf{k})^T \end{pmatrix}, \quad (2)$$

with the normal part of the Hamiltonian

$$H_0(\mathbf{k}) = (\varepsilon_{\mathbf{k}} - \mu) \mathbf{1} - JM\mathbf{n} \cdot \boldsymbol{\sigma} + \alpha_{so}\mathbf{g}(\mathbf{k}) \cdot \boldsymbol{\sigma}, \quad (3)$$

where $\boldsymbol{\sigma}$ is the pauli matrices for spin space, and $\varepsilon_{\mathbf{k}} = -t \sum_{\ell=\{x,y,z\}} \cos(k_\ell a)$ is a hopping energy with lattice constant a and the band width t . The chemical potential is denoted by μ , the exchange coupling coefficient is J , and the spin polarization is denoted by $M\mathbf{n}$ with the unit vector $\mathbf{n} = (\cos\phi \sin\theta, \sin\phi \sin\theta, \cos\theta)$. We assume the characteristic length of spatial variation to be much larger than the coherence length of superconductivity, so that $\mathbf{n}(\mathbf{r})$ can be regarded as being locally homogeneous. The effect of the inhomogeneity will be discussed in Sec. IV.

The SO coupling in a cubic lattice model can be written as

$$\mathbf{g}(\mathbf{k}) = (\sin(k_x a), \sin(k_y a), \sin(k_z a)), \quad (4)$$

which reflects the symmetry of cubic chiral magnets whose point group symmetry is T. The proximity induced superconductivity is characterized by Δ , where we take s -wave singlet

pairings. The SOC supports the proximity of the superconductivity because it causes the tilt of the spin orientation in momentum space.

III. SUPERCURRENT INDUCED SPIN POLARIZATION

In normal metals or semiconductors, current induced magnetization dynamics has been studied extensively. For non-collinear magnetic systems, one can use spin transfer torques, [30–33] which occurs from the transfer of spin angular momentum via spin polarized currents. In noncentrosymmetric systems classified into gyrotropic materials, SO coupling gives rise to an additional current-induced torque, which is called the SO torque.[34–38] One way to interpret SO torques is as follows; in gyrotropic materials, charge currents induce a spin polarization[85–88], which is known as Edelstein effect or the inverse spin-galvanic effect. This induced spin polarization acts on the magnetization as a spin-torque.

On the other hand, much less is known in superconducting states. Triplet superconductor can realize superconducting counterpart of the spin transfer torques.[48, 49, 51, 52] Related to the SO torque, it has been discussed that supercurrents produce spin polarization with Rashba spin-orbit coupling in paramagnetic state[89–94]. This paper studies chiral magnets, where the exchange coupling is large. We show that the induced polarization depends on the direction of the magnetization.

Using the BdG Hamiltonian (Eq. (2)), one can calculate the spin polarization density of the system as

$$s_\mu = \frac{1}{2} \frac{1}{V} \sum_{\mathbf{k}} n_F(\varepsilon_{n\mathbf{k}}) \langle n\mathbf{k} | \hat{S}_\mu | n\mathbf{k} \rangle, \quad (5)$$

where $|n\mathbf{k}\rangle$ and $\varepsilon_{n\mathbf{k}}$ are the eigenstates and eigenenergy of the BdG Hamiltonian with $n = 0, \dots, 3$. $n_F(\varepsilon_{n\mathbf{k}})$ is the Fermi distribution function, and V is the volume. The spin operator is given by

$$\hat{S}_\mu = \frac{\hbar}{2} \begin{pmatrix} \sigma_\mu & 0 \\ 0 & -\sigma_\mu^T \end{pmatrix}. \quad (6)$$

Now we consider a state with a finite supercurrent density $\mathbf{j} = -\frac{e}{m} n_s \hbar \mathbf{q}$ where m is an electron mass, n_s is the superfluid density, \mathbf{q} is the shift of the Fermi surface, and $-e$ is an electron charge. With a perturbation theory, the leading correction to the polarization is obtained as

$$\delta s_\mu = K_{\mu\nu} j_\nu, \quad (7)$$

where

$$K_{\mu\nu} = -\frac{m}{2e\hbar n_s} \frac{1}{V} \sum_{\mathbf{k}} \sum_{n,m} \lim_{\mathbf{q}' \rightarrow 0} \frac{n_F(\varepsilon_{n\mathbf{k}}) - n_F(\varepsilon_{m\mathbf{k}+\mathbf{q}'})}{\varepsilon_{m\mathbf{k}+\mathbf{q}'} - \varepsilon_{n\mathbf{k}}} \langle n\mathbf{k} | \hat{S}_\mu | m\mathbf{k} \rangle \langle m\mathbf{k} | \hat{V}_\nu | n\mathbf{k} \rangle, \quad (8)$$

and the velocity operator \hat{V}_μ is defined by

$$\hat{V}_\mu = \begin{pmatrix} \frac{\partial H_0}{\partial k_\mu} \Big|_{\mathbf{k}} & 0 \\ 0 & -\left(\frac{\partial H_0}{\partial k_\mu} \Big|_{-\mathbf{k}} \right)^T \end{pmatrix}. \quad (9)$$

This can be obtained from Gorkov's equation using electrons with the finite center of mass momentum [89, 95].

In the rest of this section, we first consider two limiting cases of the parameters, and show the relative orientation between the induced magnetization and applied supercurrent. Secondly, we numerically calculate the response function (Eq. (8)) with the original Hamiltonian (Eq. (2)). Finally, we discuss the spin dynamics using the obtained spin torque, and show that supercurrents can move a skyrmion in a simple manner.

A. Limiting cases

In chiral magnets, due to the large exchange splitting, $JM \gg \alpha_{so}$ is expected, but we first consider two limiting cases to provide an intuitive picture. In the limit of $JM \rightarrow 0$, the anisotropy due to the spin polarization \mathbf{n} can be neglected. In this case, symmetry argument straightforwardly leads to the relative orientation between $\delta\mathbf{s}$ and \mathbf{j} . The point group symmetry T leads to $K_{\mu\nu} = K\delta_{\mu\nu}$ [102], and we obtain

$$\delta\mathbf{s} = K\mathbf{j}, \quad (10)$$

i.e., the spin polarization is induced in parallel to the supercurrent. This relation is in contrast with the case of Rashba SO coupling (e.g., C_{4v}) that gives $\delta\mathbf{s} \propto \hat{\mathbf{z}} \times \mathbf{j}$.

In the limit of $JM \gg \alpha_{so}$, $K_{\mu\nu}$ depends on the direction of \mathbf{n} . In particular, assuming $\{JM, |\mu|\} \gg \{t, \alpha_{so}, \Delta\}$, we perform a perturbative approach. We first apply a unitary transformation $U(\mathbf{k})$ on the BdG Hamiltonian (Eq. (2)), which acts on both spin space and particle-hole space. (The detail is in Appendix A.) It diagonalizes the Hamiltonian up to the required order of a small parameter ϵ defined by $\{t, \alpha_{so}, \Delta\} \sim \epsilon JM$, and we then expand the Hamiltonian in the series of ϵ as

$$U^\dagger(\mathbf{k})H(\mathbf{k})U(\mathbf{k}) = H'_0(\mathbf{k}) + H'_1(\mathbf{k}) + \dots, \quad (11)$$

where the diagonal matrix $H'_0(\mathbf{k})$ reads

$$H'_0(\mathbf{k}) = \text{diag}(E_{0\mathbf{k}}, E_{1\mathbf{k}}, E_{2\mathbf{k}}, E_{3\mathbf{k}}) \quad (12)$$

with

$$E_{0\mathbf{k}} = \varepsilon_{\mathbf{k}} - \mu - (JM - \alpha_{so}\mathbf{g}(\mathbf{k}) \cdot \mathbf{n}), \quad (13)$$

$$E_{1\mathbf{k}} = \varepsilon_{\mathbf{k}} - \mu + (JM - \alpha_{so}\mathbf{g}(\mathbf{k}) \cdot \mathbf{n}), \quad (14)$$

$$E_{2\mathbf{k}} = -(\varepsilon_{\mathbf{k}} - \mu) + (JM + \alpha_{so}\mathbf{g}(\mathbf{k}) \cdot \mathbf{n}), \quad (15)$$

$$E_{3\mathbf{k}} = -(\varepsilon_{\mathbf{k}} - \mu) - (JM + \alpha_{so}\mathbf{g}(\mathbf{k}) \cdot \mathbf{n}), \quad (16)$$

and, every matrix element in $H'_1(\mathbf{k})$ is of the order of ϵ^2 . We consider $\mu \sim -JM$, and we project the Hilbert space to a space that is spanned by two eigenstates of $H'_0(\mathbf{k})$ with eigenenergies $E_{0\mathbf{k}}$ and $E_{2\mathbf{k}}$, noting that $E_{3\mathbf{k}} \ll \{E_{0\mathbf{k}} \sim E_{2\mathbf{k}} \sim 0\} \ll E_{1\mathbf{k}}$.

After the projection, we obtain an effective BdG Hamiltonian $H'_0(\mathbf{k}) + H'_1(\mathbf{k}) \mapsto H_{\text{eff}}(\mathbf{k})$, which is a 2×2 matrix.

We use the effective Hamiltonian $H_{\text{eff}}(\mathbf{k})$ to calculate $K_{\mu\nu}$ (Eq. (8)). The detailed structure of the quasiparticle state in this limit is analyzed in Sec. IV. We define the eigenstates of $H_{\text{eff}}(\mathbf{k})$ as $|\pm, \mathbf{k}\rangle$, whose eigenenergies are $\varepsilon_{\pm, \mathbf{k}}$. The spin and velocity operators in the projected space are defined as $U^\dagger(\mathbf{k})\hat{S}_\mu U(\mathbf{k}) \mapsto \hat{S}_\mu^{\text{eff}}$ and $U^\dagger(\mathbf{k})\hat{V}_\mu U(\mathbf{k}) \mapsto \hat{V}_\mu^{\text{eff}}$. (The detail is in Appendix B.)

For the calculation of a response against a supercurrent, the interband terms ($n \neq m$ in Eq. (8)) are important. The directional dependence of $K_{\mu\nu}$ is obtained from the matrix element:

$$S_{\mu\nu} \equiv \langle -, \mathbf{k} | \hat{S}_\mu^{\text{eff}} | +, \mathbf{k} \rangle \langle +, \mathbf{k} | \hat{V}_\nu^{\text{eff}} | -, \mathbf{k} \rangle, \quad (17)$$

$$= \frac{a^2 \hbar (JM + |\mu|)^2}{8(JM)^2 \mu^2} \frac{\alpha_{so}^3 |\Delta|^2 k_\perp^2}{|\varepsilon_{+, \mathbf{k}} - \varepsilon_{-, \mathbf{k}}|^2} n_\mu n_\nu, \quad (18)$$

$$= \langle +, \mathbf{k} | \hat{S}_\mu^{\text{eff}} | -, \mathbf{k} \rangle \langle -, \mathbf{k} | \hat{V}_\nu^{\text{eff}} | +, \mathbf{k} \rangle, \quad (19)$$

to the lowest order of ϵ , where we consider momentum region that satisfies $|\mathbf{k}|a \ll 1$ and define $k_\perp^2 = k^2 - (\mathbf{k} \cdot \mathbf{n})^2$. Integration over the momentum space as

$$K_{\mu\nu} = -\frac{m}{e\hbar n_s} \int \frac{d^3 \mathbf{k}}{(2\pi)^3} \frac{n_F(\varepsilon_{-, \mathbf{k}}) - n_F(\varepsilon_{+, \mathbf{k}})}{\varepsilon_{+, \mathbf{k}} - \varepsilon_{-, \mathbf{k}}} S_{\mu\nu}, \quad (20)$$

leads to the relation $K_{\mu\nu} = K' n_\mu n_\nu$, i.e. the induced spin polarization is given by

$$\delta\mathbf{s} = K' \mathbf{n} (\mathbf{n} \cdot \mathbf{j}), \quad (21)$$

up to the lowest order in ϵ . The spin polarization is induced in parallel to \mathbf{n} , and it is not induced when the applied supercurrent is in perpendicular to \mathbf{n} . As we will see later, this term does not produce a spin torque since the spin torque is given by $\mathbf{n} \times \delta\mathbf{s}$. In the higher order of ϵ , other terms such as the form of Eq.(10) is expected to appear and leads to the spin torque, which is important for dynamics of skyrmions discussed below.

B. Numerical results

Next, we numerically evaluate $K_{\mu\nu}$ with the BdG Hamiltonian (Eq. (2)) in the continuum model. We show the parameter dependence and the relative orientation between the induced polarization and an applied supercurrent. Fig. 2 and Fig. 3 show numerical results with the parameter: $JM = 0.5$, $t = 0.2$, $\Delta = 0.3$, $\mu = -0.9$, and the vertical axes of each figure is magnetization density per unit supercurrent density with $a = 10^{-1} \text{ nm}$ and the London penetration depth $\lambda = 50 \text{ nm}$. In Fig. 2, we first consider a spin polarization $\mathbf{n} = (0, 0, 1)$, and show the dependence of the magnitude of diagonal component, K_{xx} and K_{zz} , on α_{so}/JM . Both of them monotonically increase, and their difference represents the directional anisotropy against \mathbf{n} , which is consistent with the contribution from Eq. (21) with $\mathbf{n} = (0, 0, 1)$; the magnitude of K_{zz} becomes larger than K_{xx} in the limit of $JM \gg \alpha_{so}$.

In Fig. 3, we have fixed $\alpha_{so} = 0.1$ and show the dependence of K_{xx} and K_{zx} on the direction of \mathbf{n} which rotates in xz plane.

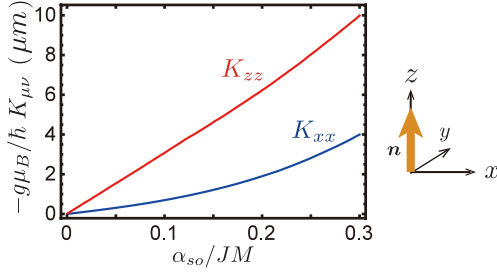


FIG. 2: Dependence of K_{xx} and K_{zz} on the parameter α_{so}/JM when the spin polarization is $\mathbf{n} = (0, 0, 1)$.

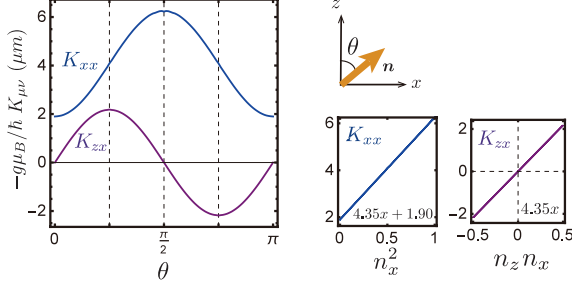


FIG. 3: Dependence of K_{xx} and K_{zx} on the direction of spin polarization $\mathbf{n} = (\sin \theta, 0, \cos \theta)$ with $0 \leq \theta \leq \pi$.

\mathbf{n} is parametrized by $0 \leq \theta \leq \pi$ as $\mathbf{n} = (\sin \theta, 0, \cos \theta)$. As is expected, the magnitude of K_{xx} and K_{zx} varies depending on θ . As shown in the bottom panels in Fig. 3, their dependence is well fitted by $K_{\mu\nu} = K^{(0)}\delta_{\mu\nu} + K^{(1)}n_\mu n_\nu$, i.e. $K_{xx} = K^{(0)} + K^{(1)}\sin^2 \theta$ and $K_{zx} = K^{(1)}\sin \theta \cos \theta$. Other components are obtained from the symmetry.

From the above results, we expect that the function of $K_{\mu\nu}$ may be interpolated between two limits given by Eq. (10) and Eq. (21) from the above results, i.e., the dependence of \mathbf{n} is expected to be the sum of Eqs.(10) and (21) for intermediate values of α_{so}/JM .

C. Equation of motion for collective coordinates

Using the obtained results, we discuss skyrmion dynamics induced by supercurrents. We consider a heterostructure system and apply a bias to realize a supercurrent flow. We neglect the effect of normal currents, which would be suppressed in the presence of superconductivity. Our analysis is based on the Landau-Lifshitz-Gilbert equation,

$$\frac{d\mathbf{n}}{dt} = -\gamma \mathbf{n} \times \mathbf{H} + \alpha_G \mathbf{n} \times \frac{d\mathbf{n}}{dt} + \mathbf{T}, \quad (22)$$

where \mathbf{n} is the direction of the magnetization, γ is the gyro-magnetic ratio, \mathbf{H} is the effective magnetic field given by the derivative of the free energy with respect to the magnetization, α_G is the Gilbert damping constant, and \mathbf{T} is a supercurrent induced spin torque. Here we focus on a spin-orbit torque that originates from the spin polarization discussed in the last section. We consider spin polarization given by the

form $\delta \mathbf{s} = K^{(0)}\mathbf{j} + K^{(1)}\mathbf{n}(\mathbf{n} \cdot \mathbf{j})$, and then we obtain spin torque:

$$\mathbf{T} = \frac{JM}{\hbar^2} \mathbf{n} \times \delta \mathbf{s}, \quad (23)$$

$$= \frac{JMK^{(0)}}{\hbar^2} \mathbf{n} \times \mathbf{j}, \quad (24)$$

i.e., only $K^{(0)}\mathbf{j}$ acts as a spin torque, and the anisotropy due to \mathbf{n} does not affect the spin torque even for large JM with the above form.

Dynamics of skyrmions is well described with the equation of motion of collective coordinates of a texture [41, 96–98]. Neglecting the deformation of skyrmions, we take the center of mass coordinate $\mathbf{R}(t)$ as the collective coordinate. The spin texture is given by $\mathbf{n}(\mathbf{r}, t) = \mathbf{n}^{sk}(\mathbf{r} - \mathbf{R}(t))$, where $\mathbf{n}^{sk}(\mathbf{r})$ is the spin configuration with a skyrmion at the origin that satisfies

$$\frac{1}{4\pi} \int d^2r \mathbf{n}^{sk} \cdot \left(\frac{\partial \mathbf{n}^{sk}}{\partial x} \times \frac{\partial \mathbf{n}^{sk}}{\partial y} \right) = -1. \quad (25)$$

As a skyrmion configuration, we take

$$n_x^{sk}(\mathbf{r}) = -\sin \Theta(r) \frac{y}{r}, \quad (26)$$

$$n_y^{sk}(\mathbf{r}) = \sin \Theta(r) \frac{x}{r}. \quad (27)$$

$$n_z^{sk}(\mathbf{r}) = \cos \Theta(r), \quad (28)$$

where $\Theta(r)$ only depends on $r = \sqrt{x^2 + y^2}$, and it satisfied $\Theta(0) = \pi$ and $\Theta(\infty) = 0$. With this configuration and the torque (Eq. (24)), we calculate the time dependence of $\mathbf{R}(t)$ from the LLG equation (Eq. (22)).

$$\dot{R}_x = -\Lambda_0 j_x + \alpha_G \Lambda_1 j_y, \quad (29)$$

$$\dot{R}_y = -\Lambda_0 j_y - \alpha_G \Lambda_1 j_x, \quad (30)$$

where

$$\Lambda_0 = \frac{JMK^{(0)}}{\hbar^2} \frac{L_0}{4\pi}, \quad (31)$$

$$\Lambda_1 = \frac{JMK^{(0)}}{\hbar^2} \frac{\Gamma_0 L_0}{16\pi^2}. \quad (32)$$

L_0 and Γ_0 depends on the function $\Theta(r)$; $L_0 = \int d^2r \partial_x \mathbf{n} \cdot \partial_y \mathbf{n} = -\int d^2r \partial_y \mathbf{n} \cdot \partial_x \mathbf{n}$ is of the order of the radius of a skyrmion, and $\Gamma_0 = \int d^2r \partial_x \mathbf{n} \cdot \partial_x \mathbf{n} = \int d^2r \partial_y \mathbf{n} \cdot \partial_y \mathbf{n}$.

The supercurrent-induced torque can give rise to the drift motion of skyrmions, and the finite Gilbert damping coefficient α_G gives the transverse motion against the supercurrent, which is a well known effect for skyrmion dynamics[26]. Eqs. (29) and (30) are compatible with the results obtained from phenomenological arguments in the presence of SO coupling. [41]

IV. QUASIPARTICLE STRUCTURE

In the heterostructure of interest, Bogoliubov quasiparticles have nontrivial band topology; a pair of Weyl points exists.

We first study the effective Hamiltonian which describes low-energy quasiparticles, and then numerically demonstrate the existence of type-I and type-II Weyl points. In the end of this section, we discuss the effect of the spatial inhomogeneity in spin textures and show that an effective magnetic field may act on the quasiparticles.

A. Type-I and Type-II Weyl fermions

The structure of Bogoliubov quasiparticles in the case with spin textures such as skyrmions is rather complicated. Thus, before tackling this problem, we first consider the case of a homogeneous exchange field. This analysis is valid provided that the spatial variation of the spin texture is sufficiently slow compared to the Fermi wave-length, and thus the spin configuration is locally approximated by a homogeneous structure.

For a homogeneous spin configuration, the effective Hamiltonian is derived in Sec. III A. The Hamiltonian for low-energy Bogoliubov quasiparticles in the limit of $\{JM, |\mu|\} \gg \{t, \alpha_{so}, \Delta\}$ with the condition $\mu \sim -JM$ is given by

$$H_{\text{eff}}(\mathbf{k}) = \alpha_{so} \mathbf{k} \cdot \mathbf{n} \mathbf{1} + \begin{pmatrix} \xi_{\text{eff}}(\mathbf{k}) & \Delta_{\text{eff}} \gamma \cdot \mathbf{k} \\ \Delta_{\text{eff}} \gamma^* \cdot \mathbf{k} & -\xi_{\text{eff}}(\mathbf{k}) \end{pmatrix} \quad (33)$$

where

$$\Delta_{\text{eff}} = \frac{|\Delta| \alpha_{so} (JM + |\mu|)}{2JM|\mu|}, \quad (34)$$

$$\xi_{\text{eff}}(\mathbf{k}) = \varepsilon_{\mathbf{k}} - JM - \mu - \frac{|\Delta|^2}{2\mu} + \frac{\alpha_{so}^2}{2JM} k_{\perp}^2. \quad (35)$$

Here we consider the momentum $|\mathbf{k}|a \ll 1$ ($a=1$), and define $k_{\perp}^2 = k^2 - (\mathbf{k} \cdot \mathbf{n})^2$. A complex vector $\gamma = (\gamma_x, \gamma_y, \gamma_z)$ satisfies $|Re\gamma| = |Im\gamma| = 1$ and $Re\gamma \times Im\gamma = -\mathbf{n}$. (See Appendix A for detail)

The two bands cross at $\mathbf{k} = \pm k_0 \mathbf{n}$ if there exists k_0 that satisfies $\xi_{\text{eff}}(k_0 \mathbf{n}) = 0$, and the crossing points are shifted from the zero energy by $\pm \alpha_{so} k_0$. These crossing points are not gapped out in the presence of the spin rotation symmetry along \mathbf{n} , i.e., two crossing bands of interest have different eigenvalues of $\hat{\mathbf{S}} \cdot \mathbf{n}$, which commutes with $H(k_0 \mathbf{n})$.

Without loss of generality, we can define x, y and z axis of momentum along $Re\gamma, Im\gamma$, and \mathbf{n} . The effective Hamiltonian around the crossing points reads

$$H_{\text{eff}}(\pm k_0 \hat{\mathbf{z}} + \mathbf{q}) = \alpha_{so}(\pm k_0 + q_z) \mathbf{1} + \begin{pmatrix} \pm t k_0 q_z & \Delta_{\text{eff}}(q_x + i q_y) \\ \Delta_{\text{eff}}(q_x - i q_y) & \mp t k_0 q_z \end{pmatrix}. \quad (36)$$

Each cone is tilted by $\alpha_{so} q_z$, and numerical calculations of the Berry curvature with the original BdG Hamiltonian (Eq. (2)) show that they are a pair of Weyl points, which are a source and a sink of the Berry curvature. The numerical result of the phase diagram is summarized in Fig. 4 for the parameter $JM = 0.5$, $t = 0.2$, $\Delta = 0.3$. For the chemical potential $\mu > -1.0$, a pair of Weyl points with the opposite topological charge exists. In Fig. 5 (a) and (b), a band structure for the parameter $\mu = -0.9$, $\alpha_{so}/JM = 0.2$ is shown, which has

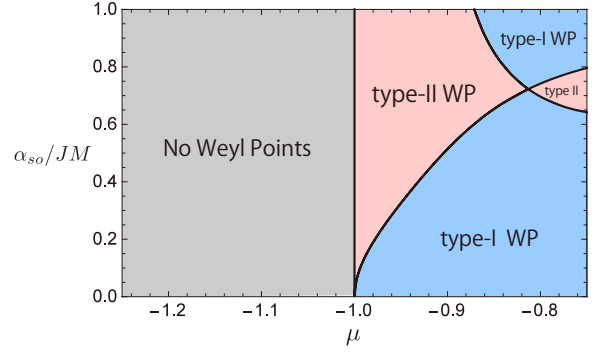


FIG. 4: Phase diagram of Weyl points (WP) as a function of chemical potential μ and α_{so}/JM with the parameter $JM = 0.5$, $t = 0.2$, $\Delta = 0.3$. There are no Weyl points for $\mu < -1.0$. In phases denoted by type-I (type-II) WP, a pair of type-I (type-II) Weyl points exist.

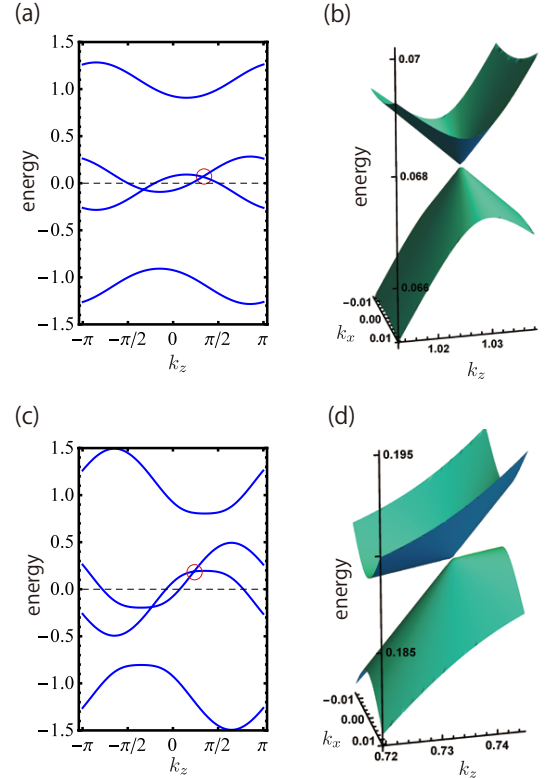


FIG. 5: Energy spectrum for chemical potential $\mu = -0.9$. The crossing points locate at $\mathbf{k} = (0, 0, \pm k_0)$. (a), (b) Energy spectrum in $k_x = k_y = 0$ and in k_z k_x plane with the parameter $\alpha_{so}/JM = 0.2$. A pair of type-I Weyl cones exists in the bands of quasiparticles. (c), (d) Energy spectrum in $k_x = k_y = 0$ and in k_z k_x plane with the parameter $\alpha_{so}/JM = 0.8$. A pair of type-II Weyl cones exist.

conventional (type-I) Weyl cones. The dispersions are weakly tilted in k_z direction.

Interestingly, changing α_{so}/JM leads to a transition between type-I and type-II Weyl cones. Type-II Weyl cones are characterized by the finite density of states at the crossing energy due to the tilt of the cones. Type-II Weyl cones are shown

in Fig. 5 (c) and (d) for $JM = 0.5$, $t = 0.2$, $\Delta = 0.3$. This tilt may induce distinct property in transport due to the anomaly, which may be realized by an effective magnetic field discussed in the next section.

The surface Majorana arc exists for both type-I and type-II Weyl points as shown in Fig. 6. The surface state in Fig. 6 are obtained by numerical calculations with an open boundary in y direction, and the zero energy states are plotted in k_z k_x plane. The red region denotes the states localized on one of the surfaces. Since the positions of the Weyl points is at $\pm k_0 \mathbf{n}$, the surface plane in which the localized states appear can be changed by the direction of the magnetization.

For $k_z = 0, \pm\pi$ plane, our system can be mapped to a well-known model. By rotating the momentum by 90° along k_z axis, the Hamiltonian (Eq. (2)) is equivalent to a model to realize a spinless $p + ip$ superconductor with the Rashba SO coupling[64, 65]. These two-dimensional planes can have nonzero Chern number depending on the effective chemical potential, and the difference of the Chern number ensures the existence of Weyl points.

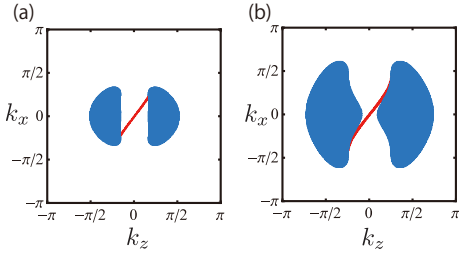


FIG. 6: Zero energy states when the system has an open boundary in y -direction. The gapless states in the bulk are indicated by the blue regions. The states localized at one boundary are highlighted in red. (a) $\alpha_{so}/JM = 0.2$ (b) $\alpha_{so}/JM = 0.8$.

B. Inhomogeneous spin texture

So far, we have studied a locally homogeneous system assuming that the spin texture varies weakly enough in space. Now we include the effect of inhomogeneity to the lowest order, and show the emergence of an effective magnetic field. We consider quasiparticle states around some arbitrary point \mathbf{r}_0 , and we define $\mathbf{n}(\mathbf{r}_0) = \mathbf{n}_0$ and $\gamma(\mathbf{r}_0) = \gamma_0$. We then rewrite as $\mathbf{n}(\mathbf{r}) = \mathbf{n}_0 + \delta\mathbf{n}(\mathbf{r})$ and $\gamma(\mathbf{r}) = \gamma_0 + \delta\gamma(\mathbf{r})$. Around a Weyl point at \mathbf{r}_0 given by $\mathbf{k} = k_0 \mathbf{n}_0$, we define the Bogoliubov quasiparticle operator as $\psi(\mathbf{r}) = e^{ik_0 \mathbf{n}_0 \cdot \mathbf{r}} \tilde{\psi}_+(\mathbf{r})$. Up to the lowest order of spatial variation, the Hamiltonian for slowly

varying field is given by

$$H_{\text{eff}}^+(\mathbf{r}) = \alpha_{so}(k_0 + \mathbf{n}_0 \cdot \hat{\mathbf{p}})1 + \begin{pmatrix} tk_0 \mathbf{n}_0 \cdot \hat{\mathbf{p}} & \Delta_{\text{eff}} \gamma_0 \cdot (\hat{\mathbf{p}} - k_0 \mathbf{n}(\mathbf{r})) \\ \Delta_{\text{eff}} \gamma_0^* \cdot (\hat{\mathbf{p}} - k_0 \mathbf{n}(\mathbf{r})) & -tk_0 \mathbf{n}_0 \cdot \hat{\mathbf{p}} \end{pmatrix}, \quad (37)$$

$$= \alpha_{so}(k_0 + \mathbf{n}_0 \cdot (\hat{\mathbf{p}} - k_0 \delta\mathbf{n}(\mathbf{r})))1 + \begin{pmatrix} tk_0 \mathbf{n}_0 \cdot (\hat{\mathbf{p}} - k_0 \delta\mathbf{n}(\mathbf{r})) & \Delta_{\text{eff}} \gamma_0 \cdot (\hat{\mathbf{p}} - k_0 \delta\mathbf{n}(\mathbf{r})) \\ \Delta_{\text{eff}} \gamma_0^* \cdot (\hat{\mathbf{p}} - k_0 \delta\mathbf{n}(\mathbf{r})) & -tk_0 \mathbf{n}_0 \cdot (\hat{\mathbf{p}} - k_0 \delta\mathbf{n}(\mathbf{r})) \end{pmatrix}, \quad (38)$$

where we have used the relation $\mathbf{n}(\mathbf{r}) \cdot \gamma(\mathbf{r}) = 0$ and $\mathbf{n}_0 \cdot \delta\mathbf{n}(\mathbf{r}) = 0$. Minimal coupling $\hat{\mathbf{p}} - k_0 \delta\mathbf{n}(\mathbf{r})$ exhibits that the effect of the spatial variation of spins can be described by the effective magnetic field given by $B_{\text{eff}}(\mathbf{r}) = k_0 \nabla \times \mathbf{n}(\mathbf{r})$. Around the other Weyl point at $-k_0 \mathbf{n}_0$, the sign is the opposite: $B_{\text{eff}}(\mathbf{r}) = -k_0 \nabla \times \mathbf{n}(\mathbf{r})$.

This result shows that Bogoliubov quasiparticles around each Weyl cone may form the Landau levels in the presence of the spin texture with $\nabla \times \mathbf{n}(\mathbf{r}) \neq 0$, and the chiral zero modes are expected to appear for each cone, which is studied in the A phase of ^3He [99–101]. The velocities of the chiral zero modes have the same direction for two cones to preserve the particle hole symmetry, and they are along the direction of $\nabla \times \mathbf{n}(\mathbf{r})$.

A skyrmion texture gives $\nabla \times \mathbf{n}(\mathbf{r}) \neq 0$, and a skyrmion flow is expected to cause an effective electric field given by $\mp k_0 \partial_t \mathbf{n}$, which acts on quasiparticles in each cone. As has been discussed in ^3He [100, 101], the spectral flow in the chiral zero mode causes the excitation of quasiparticles, and the back-reaction gives rise to a force acting on the skyrmion, which is in perpendicular to the velocity of the skyrmion [103], i.e., the anomaly of Weyl fermions can affect the skyrmion dynamics.

Tuning the tilt is expected to change the property of the chiral zero modes, as is studied in Weyl semimetal[83], and consequently the sign of the force on a skyrmion may be changed by tuning the tilt. We leave the detailed study of skyrmion dynamics associated with Weyl fermions in chiral magnet for future work.

V. SUMMARY AND DISCUSSION

In this paper, we have studied a spin-torque induced by a supercurrent in a heterostructure composed of a cubic chiral magnet and an s -wave superconductor. Due to the exchange coupling, the spin polarization induced by a supercurrent depends on the direction of the magnetization. From the numerical and analytical calculation, we expect that such anisotropy does not change the torque, and a supercurrent can induce a skyrmion flow in a simple manner. We have also pointed out the existence of a pair of Weyl points in the quasiparticle bands. The positions of the Weyl points are determined by the magnetization, and the resulting effective electromagnetic field may give rise to novel phenomena in spintronics. The tilt of the cones can also be changed by the strength of the

SO coupling, and type-II Weyl points may be realized. We believe that nontrivial band topology of Bogoliubov quasiparticles provides a new perspective in superconducting spintronics.

We leave the discussion on the stability of the proximity-induced superconducting gap for future work. The quantitative estimation requires self-consistent calculations of the superconducting gap. However, at this point, we expect that there should be a finite region where the superconducting gap is proximity-induced in the chiral magnet when the interface between the superconductor and the chiral magnet is sufficiently smooth.

Appendix A: Effective Hamiltonian

In this appendix, we show the derivation of the effective Hamiltonian when $\{JM, |\mu|\} \gg \{t, \alpha_{so}, \Delta\}$. We start from the BdG Hamiltonian in Eq. (2). Then we apply a unitary transformation $U^\dagger(\mathbf{k})H(\mathbf{k})U(\mathbf{k})$. The unitary matrix is given by

$$U(\mathbf{k}) = \begin{pmatrix} U_0 & 0 \\ 0 & U_0^* \end{pmatrix} e^{iQ(\mathbf{k})}, \quad (\text{A1})$$

where U_0 rotates the spin axis as $U_0^\dagger \mathbf{n} \cdot \boldsymbol{\sigma} U_0 = \sigma_z$.

$Q(\mathbf{k})$ is Hermite matrix given by

$$Q(\mathbf{k}) = \begin{pmatrix} 0 & -\frac{i\alpha_{so}}{2M}\omega & 0 & -\frac{i\Delta}{2\mu} \\ \frac{i\alpha_{so}}{2M}\omega^* & 0 & \frac{i\Delta}{2\mu} & 0 \\ 0 & -\frac{i\Delta^*}{2\mu} & 0 & \frac{i\alpha_{so}}{2M}\omega^* \\ \frac{i\Delta^*}{2\mu} & 0 & -\frac{i\alpha_{so}}{2M}\omega & 0 \end{pmatrix} \quad (\text{A2})$$

with

$$\omega = \sum_{\ell=x,y,z} \sin(k_\ell a) (U_0^\dagger \sigma_\ell U_0)_{12}. \quad (\text{A3})$$

Then we expand the Hamiltonian in the series of ϵ where we define the small parameter by $\{t, \alpha_{so}, \Delta\} \sim \epsilon JM$, as $U^\dagger(\mathbf{k})H(\mathbf{k})U(\mathbf{k}) = H'_0(\mathbf{k}) + H'_1(\mathbf{k}) + O(\epsilon^3)$, where $H'_0(\mathbf{k})$ is given by Eq. (12) and

$$H'_1(\mathbf{k}) = \begin{pmatrix} -\frac{|\Delta|^2}{2\mu} - \frac{\alpha_{so}^2}{2JM}|\omega|^2 & \frac{\alpha_{so}^2}{JM}\beta\omega & u_0\Delta\omega & \frac{\Delta}{\mu}(\epsilon_{\mathbf{k}} + \alpha_{so}\beta) \\ \frac{\alpha_{so}^2}{JM}\beta\omega^* & -\frac{|\Delta|^2}{2\mu} + \frac{\alpha_{so}^2}{2JM}|\omega|^2 & -\frac{\Delta}{\mu}(\epsilon_{\mathbf{k}} - \alpha_{so}\beta) & u_1\Delta\omega^* \\ u_0\Delta^*\omega^* & -\frac{\Delta^*}{\mu}(\epsilon_{\mathbf{k}} - \alpha_{so}\beta) & \frac{|\Delta|^2}{2\mu} + \frac{\alpha_{so}^2}{2JM}|\omega|^2 & -\frac{\alpha_{so}^2}{JM}\beta\omega^* \\ \frac{\Delta^*}{\mu}(\epsilon_{\mathbf{k}} + \alpha_{so}\beta) & u_1\Delta^*\omega & -\frac{\alpha_{so}^2}{JM}\beta\omega & \frac{|\Delta|^2}{2\mu} - \frac{\alpha_{so}^2}{2JM}|\omega|^2 \end{pmatrix}, \quad (\text{A4})$$

with $\beta = \sum_{\ell=x,y,z} \sin(k_\ell a) n_\ell$, $u_0 = -\frac{\alpha_{so}(JM-\mu)}{2JM\mu}$, and $u_1 = \frac{\alpha_{so}(JM+\mu)}{2JM\mu}$. When $\mu \sim -JM$, the eigenstates of $H'_0(\mathbf{k})$ are energetically separated as $E_{3\mathbf{k}} \ll \{E_{0\mathbf{k}} \sim E_{2\mathbf{k}} \sim 0\} \ll E_{1\mathbf{k}}$. We project the Hilbert space to a space around zero energy, i.e. a space spanned by eigenstates with eigenenergy $E_{0\mathbf{k}}$ and $E_{2\mathbf{k}}$.

The effective Hamiltonian $H_{\text{eff}}(\mathbf{k})$ is given by

$$H_{\text{eff}}(\mathbf{k}) = \begin{pmatrix} (H'_0(\mathbf{k}))_{11} + (H'_1(\mathbf{k}))_{11} & (H'_0(\mathbf{k}))_{13} + (H'_1(\mathbf{k}))_{13} \\ (H'_0(\mathbf{k}))_{31} + (H'_1(\mathbf{k}))_{31} & (H'_0(\mathbf{k}))_{33} + (H'_1(\mathbf{k}))_{33} \end{pmatrix}, \quad (\text{A5})$$

$$= \begin{pmatrix} E_{0\mathbf{k}} - \frac{|\Delta|^2}{2\mu} - \frac{\alpha_{so}^2}{2JM}|\omega|^2 & -\frac{\alpha_{so}|\Delta|(JM-\mu)}{2JM\mu}e^{i\varphi}\omega \\ -\frac{\alpha_{so}|\Delta|(JM-\mu)}{2JM\mu}e^{-i\varphi}\omega^* & E_{2\mathbf{k}} + \frac{|\Delta|^2}{2\mu} + \frac{\alpha_{so}^2}{2JM}|\omega|^2 \end{pmatrix}, \quad (\text{A6})$$

where we define $\Delta = |\Delta|e^{i\varphi}$. We introduce a complex vector $\gamma = (\gamma_x, \gamma_y, \gamma_z)$ as

$$\gamma = e^{i\varphi} (U_0^\dagger \boldsymbol{\sigma} U_0)_{12}, \quad (\text{A7})$$

where $(U_0^\dagger \boldsymbol{\sigma} U_0)_{12}$ is the $(1, 2)$ component in the 2×2 matrix $U_0^\dagger \boldsymbol{\sigma} U_0$. One can show the following relations

$$|Re\gamma| = |Im\gamma| = 1, \quad (\text{A8})$$

$$Re\gamma \cdot Im\gamma = 0, \quad (\text{A9})$$

$$Re\gamma \times Im\gamma = -\mathbf{n}, \quad (\text{A10})$$

$$\epsilon_{\mu\nu\lambda} \partial_\mu (\gamma^* \cdot \partial_\nu \gamma) = -2i\epsilon_{\mu\nu\lambda} \mathbf{n} \cdot (\partial_\mu \mathbf{n} \times \partial_\nu \mathbf{n}). \quad (\text{A11})$$

The last equation shows that the rotation of the superfluid velocity is given by the skyrmion density. Around the Γ point ($|\mathbf{k}|a \ll 1$), we obtain the effective Hamiltonian in Eq. (33), noting that $e^{i\varphi}\omega = \gamma \cdot \mathbf{k}a$ and $|\omega|^2 = a^2k^2 - a^2(\mathbf{k} \cdot \mathbf{n})^2$.

Appendix B: Edelstein effect with the effective Hamiltonian

In this section, we calculate the matrix element $S_{\mu\nu}$ (Eq. (17)) with the effective Hamiltonian in the continuum limit ($|k|a \ll 1$). The effective Hamiltonian (Eq. (33)) is

$$H_{\text{eff}}(\mathbf{k}) = f_0 \mathbf{1} + \mathbf{f} \cdot \boldsymbol{\tau}, \quad (\text{B1})$$

with $\boldsymbol{\tau} = (\tau_x, \tau_y, \tau_z)$ are pauli matrices, and

$$f_0 = \alpha_{so} \mathbf{k} \cdot \mathbf{n}, \quad (\text{B2})$$

$$\mathbf{f} = (f_1, f_2, f_3), \quad (\text{B3})$$

$$f_1 = \Delta_{\text{eff}} \text{Re} \boldsymbol{\gamma} \cdot \mathbf{k}, \quad (\text{B4})$$

$$f_2 = -\Delta_{\text{eff}} \text{Im} \boldsymbol{\gamma} \cdot \mathbf{k}, \quad (\text{B5})$$

$$f_3 = \xi_{\text{eff}}(\mathbf{k}). \quad (\text{B6})$$

We define $\mathbf{f}/|\mathbf{f}| = (\sin \theta_0 \cos \phi_0, \sin \theta_0 \sin \phi_0, \cos \theta_0)$, and then the eigenstates of Eq. (33) are given by

$$|+, \mathbf{k}\rangle = \begin{pmatrix} \cos \frac{\theta_0}{2} e^{-i\phi_0} \\ \sin \frac{\theta_0}{2} \end{pmatrix}, \quad (\text{B7})$$

$$|-, \mathbf{k}\rangle = \begin{pmatrix} \sin \frac{\theta_0}{2} e^{-i\phi_0} \\ -\cos \frac{\theta_0}{2} \end{pmatrix}. \quad (\text{B8})$$

The corresponding eigenstates are $\varepsilon_{\pm, \mathbf{k}} = f_0 \pm |\mathbf{f}|$, which depend on k^2 and $\mathbf{k} \cdot \mathbf{n}$. The spin and velocity operators in the projected space are

$$\hat{S}_{\mu}^{\text{eff}} \sim \frac{\hbar}{2} \left(n_{\mu} \tau_z - \frac{\alpha_{so}}{M} \text{Re}(\gamma_{\mu}^* \boldsymbol{\gamma} \cdot \mathbf{k}) \mathbf{1} \right), \quad (\text{B9})$$

$$\hat{V}_{\mu}^{\text{eff}} \sim -\hbar k_{\mu} \mathbf{1} + \alpha_{so} n_{\mu} \tau_z, \quad (\text{B10})$$

where we have expanded in the series of ϵ . Thus we obtain

$$S_{\mu\nu} = \langle -, \mathbf{k} | \hat{S}_{\mu}^{\text{eff}} | +, \mathbf{k} \rangle \langle +, \mathbf{k} | \hat{V}_{\nu}^{\text{eff}} | -, \mathbf{k} \rangle, \quad (\text{B11})$$

$$= \langle -, \mathbf{k} | \tau_z | +, \mathbf{k} \rangle \langle +, \mathbf{k} | \tau_z | -, \mathbf{k} \rangle \frac{\hbar}{2} \alpha_{so} n_{\mu} n_{\nu}, \quad (\text{B12})$$

$$= \sin^2 \theta_0 \frac{\hbar}{2} \alpha_{so} n_{\mu} n_{\nu}, \quad (\text{B13})$$

$$= \frac{\Delta_{\text{eff}}^2 k_{\perp}^2}{\xi_{\text{eff}}(\mathbf{k})^2 + \Delta_{\text{eff}}^2 k_{\perp}^2} \frac{\hbar}{2} \alpha_{so} n_{\mu} n_{\nu}, \quad (\text{B14})$$

where $k_{\perp}^2 = k^2 - (\mathbf{k} \cdot \mathbf{n})^2$. One can also show that $\langle +, \mathbf{k} | \hat{S}_{\mu}^{\text{eff}} | -, \mathbf{k} \rangle \langle -, \mathbf{k} | \hat{V}_{\nu}^{\text{eff}} | +, \mathbf{k} \rangle = S_{\mu\nu}$.

Acknowledgments

We thank Muhammad Shahbaz Anwar, Alexander Baltas, Akito Daido, Takuya Nomoto, Masatoshi Sato, Yuki Shiomi, and Yoichi Yanase for fruitful discussion. This work was supported by the Grant-in-Aids for Scientific Research from MEXT of Japan [Grants No. 23540406, No. 25220711, and No. 15H05852 (KAKENHI on Innovative Areas Topological Materials Science)]. R. T. is supported by a JSPS Fellowship for Young Scientists.

-
- [1] M. Z. Hasan and C. L. Kane, Rev. Mod. Phys. **82**, 3045 (2010).
 - [2] X. L. Qi and S. C. Zhang, Rev. Mod. Phys. **83**, 1057 (2011).
 - [3] G. E. Volovik, *The universe in a helium droplet* (Oxford University Press, Oxford, 2003).
 - [4] S. Murakami, New J. Phys. **9**, 356 (2007).
 - [5] X. Wan, A. M. Turner, A. Vishwanath, and S. Y. Savrasov, Phys. Rev. B **83**, 205101 (2011).
 - [6] G. Xu, H. Weng, Z. Wang, X. Dai, and Z. Fang, Phys. Rev. Lett. **107**, 186806 (2011).
 - [7] K. Y. Yang, Y. M. Lu, and Y. Ran, Phys. Rev. B **84**, 12 (2011).
 - [8] A. A. Burkov and L. Balents, Phys. Rev. Lett. **107**, 127205 (2011).
 - [9] G. B. Halász and L. Balents, Phys. Rev. B **85**, 035103 (2012).
 - [10] W. Witczak-Krempa and Y. B. Kim, Phys. Rev. B **85**, 045124 (2012).
 - [11] P. Hosur, S. A. Parameswaran, and A. Vishwanath, Phys. Rev. Lett. **108**, 046602 (2012).
 - [12] A. A. Zyuzin and A. A. Burkov, Phys. Rev. B **86**, 115133 (2012).
 - [13] V. Aji, Phys. Rev. B **85**, 241101 (2012).
 - [14] D. T. Son and N. Yamamoto, Phys. Rev. Lett. **109**, 181602 (2012).
 - [15] C.-X. Liu, P. Ye, and X.-L. Qi, Phys. Rev. B **87**, 235306 (2013).
 - [16] U. K. Rössler, A. N. Bogdanov, and C. Pfleiderer, Nature **442**, 797 (2006).
 - [17] S. Mühlbauer, B. Binz, F. Jonietz, C. Pfleiderer, A. Rosch, A. Neubauer, R. Georgii, and P. Böni, Science **323**, 915 (2009).
 - [18] X. Z. Yu, Y. Onose, N. Kanazawa, J. H. Park, J. H. Han, Y. Matsui, N. Nagaosa, and Y. Tokura, Nature **465**, 901 (2010).
 - [19] W. Münzer, A. Neubauer, T. Adams, S. Mühlbauer, C. Franz, F. Jonietz, R. Georgii, P. Böni, B. Pedersen, M. Schmidt, A. Rosch, and C. Pfleiderer, Phys. Rev. B **81**, 041203 (2010).
 - [20] X. Z. Yu, N. Kanazawa, Y. Onose, K. Kimoto, W. Z. Zhang, S. Ishiwata, Y. Matsui, and Y. Tokura, Nat. Mater. **10**, 106 (2011).
 - [21] N. Nagaosa and Y. Tokura, Nat. Nanotechnol. **8**, 899 (2013).
 - [22] M. Stone, Phys. Rev. B **53**, 16573 (1996).
 - [23] G. Volovik, J. Phys. C Solid State Phys. **20**, L83 (1987).
 - [24] F. Jonietz, S. Mühlbauer, C. Pfleiderer, A. Neubauer, W. Münzer, A. Bauer, T. Adams, R. Georgii, P. Böni, R. a. Duine, K. Everschor, M. Garst, and A. Rosch, Science **330**, 1648 (2010).
 - [25] X. Yu, N. Kanazawa, W. Zhang, T. Nagai, T. Hara, K. Kimoto, Y. Matsui, Y. Onose, and Y. Tokura, Nat. Commun. **3**, 988 (2012).

- [26] J. Iwasaki, M. Mochizuki, and N. Nagaosa, *Nat. Nanotechnol.* **8**, 742 (2013).
- [27] A. Fert, V. Cros, and J. Sampaio, *Nat. Nanotechnol.* **8**, 152 (2013).
- [28] S.-Z. Lin, C. Reichhardt, C. D. Batista, and A. Saxena, *Phys. Rev. B* **87**, 214419 (2013).
- [29] C. Schutte, J. Iwasaki, A. Rosch, and N. Nagaosa, *Phys. Rev. B* **90**, 174434 (2014).
- [30] J. Slonczewski, *J. Magn. Magn. Mater.* **159**, L1 (1996).
- [31] J. Slonczewski, *J. Magn. Magn. Mater.* **195**, L261 (1999).
- [32] L. Berger, *Phys. Rev. B* **54**, 9353 (1996).
- [33] L. Berger, *Phys. Rev. B* **59**, 11465 (1999).
- [34] A. Chernyshov, M. Overby, X. Liu, J. K. Furdyna, Y. Lyanda-Geller, and L. P. Rokhinson, *Nat. Phys.* **5**, 656 (2008).
- [35] A. Manchon and S. Zhang, *Phys. Rev. B* **78**, 212405 (2008).
- [36] I. Garate and A. H. MacDonald, *Phys. Rev. B* **80**, 134403 (2009).
- [37] I. M. Miron, G. Gaudin, S. Auffret, B. Rodmacq, A. Schuhl, S. Pizzini, J. Vogel, and P. Gambardella, *Nat. Mater.* **9**, 230 (2010).
- [38] L. Liu, O. J. Lee, T. J. Gudmundsen, D. C. Ralph, and R. A. Buhrman, *Phys. Rev. Lett.* **109**, 096602 (2012).
- [39] A. V. Khvalkovskiy, V. Cros, D. Apalkov, V. Nikitin, M. Krounbi, K. A. Zvezdin, A. Anane, J. Grollier, and A. Fert, *Phys. Rev. B* **87**, 020402 (2013).
- [40] K. M. D. Hals and A. Brataas, *Phys. Rev. B* **87**, 174409 (2013).
- [41] K. M. D. Hals and A. Brataas, *Phys. Rev. B* **89**, 064426 (2014).
- [42] F. S. Bergeret, A. F. Volkov, and K. B. Efetov, *Phys. Rev. Lett.* **86**, 4096 (2001).
- [43] X. Waintal and P. W. Brouwer, *Phys. Rev. B* **65**, 054407 (2002).
- [44] F. S. Bergeret, A. F. Volkov, and K. B. Efetov, *Rev. Mod. Phys.* **77**, 1321 (2005).
- [45] R. S. Keizer, S. T. B. Goennenwein, T. M. Klapwijk, G. Miao, G. Xiao, and A. Gupta, *Nature* **439**, 825 (2006).
- [46] M. Eschrig and T. Löfwander, *Nat. Phys.* **4**, 138 (2008).
- [47] E. Zhao and J. A. Sauls, *Phys. Rev. B* **78**, 174511 (2008).
- [48] V. Braude and Y. M. Blanter, *Phys. Rev. Lett.* **100**, 207001 (2008).
- [49] F. Konschelle and A. Buzdin, *Phys. Rev. Lett.* **102**, 017001 (2009).
- [50] M. Eschrig, *Phys. Today* **64**, 43 (2011).
- [51] J. Linder and T. Yokoyama, *Phys. Rev. B* **83**, 012501 (2011).
- [52] P. Sacramento, L. Fernandes Silva, G. Nunes, M. Araújo, and V. Vieira, *Phys. Rev. B* **83**, 054403 (2011).
- [53] J. Linder, A. Brataas, Z. Shomali, and M. Zareyan, *Phys. Rev. Lett.* **109**, 237206 (2012).
- [54] F. S. Bergeret and I. V. Tokatly, *Phys. Rev. Lett.* **110**, 117003 (2013).
- [55] F. S. Bergeret and I. V. Tokatly, *Phys. Rev. B* **89**, 134517 (2014).
- [56] I. Kulagina and J. Linder, *Phys. Rev. B* **90**, 054504 (2014).
- [57] K. Halterman, O. T. Valls, and C.-T. Wu, *Phys. Rev. B* **92**, 174516 (2015).
- [58] J. Linder and J. W. A. Robinson, *Nat. Phys.* **11**, 307 (2015).
- [59] M. Eschrig, *Rep. Prog. Phys.* **78**, 104501 (2015).
- [60] S. H. Jacobsen, J. A. Ouassou, and J. Linder, *Phys. Rev. B* **92**, 024510 (2015).
- [61] T. Yokoyama and J. Linder, *Phys. Rev. B* **92**, 060503 (2015).
- [62] K. M. D. Hals, *Phys. Rev. B* **93**, 115431 (2016).
- [63] S. Fujimoto, *Phys. Rev. B* **77**, 220501 (2008).
- [64] M. Sato, Y. Takahashi, and S. Fujimoto, *Phys. Rev. Lett.* **103**, 020401 (2009).
- [65] J. D. Sau, R. M. Lutchyn, S. Tewari, and S. Das Sarma, *Phys. Rev. Lett.* **104**, 040502 (2010).
- [66] S. S. Pershoguba, K. Björnson, A. M. Black-Schaffer, and A. V. Balatsky, *Phys. Rev. Lett.* **115**, 116602 (2015).
- [67] K. Björnson, S. S. Pershoguba, A. V. Balatsky, and A. M. Black-Schaffer, *Phys. Rev. B* **92**, 214501 (2015).
- [68] S. Nakosai, Y. Tanaka, and N. Nagaosa, *Phys. Rev. B* **88**, 180503 (2013).
- [69] J. Klinovaja, P. Stano, A. Yazdani, and D. Loss, *Phys. Rev. Lett.* **111**, 186805 (2013).
- [70] W. Chen and A. P. Schnyder, *Phys. Rev. B* **92**, 214502 (2015).
- [71] J. Li, T. Neupert, Z. Wang, A. H. MacDonald, A. Yazdani, and B. A. Bernevig, *Nat. Commun.* **7**, 12297 (2016).
- [72] S.-Y. Xu, N. Alidoust, G. Chang, H. Lu, B. Singh, I. Belopolski, D. Sanchez, X. Zhang, G. Bian, H. Zheng, M.-A. Hsuanu, Y. Bian, S.-M. Huang, C.-H. Hsu, T.-R. Chang, H.-T. Jeng, A. Bansil, V. N. Strocov, H. Lin, S. Jia, and M. Z. Hasan, , arXiv:1603.07318 .
- [73] L. Huang, T. M. McCormick, M. Ochi, Z. Zhao, M. Suzuki, R. Arita, Y. Wu, D. Mou, H. Cao, J. Yan, N. Trivedi, and A. Kaminski, arXiv:1603.06482 .
- [74] N. Xu, Z. J. Wang, A. P. Weber, A. Magrez, P. Bugnon, H. Berger, C. E. Matt, J. Z. Ma, B. B. Fu, B. Q. Lv, N. C. Plumb, M. Radovic, E. Pomjakushina, K. Conder, T. Qian, J. H. Dil, J. Mesot, H. Ding, and M. Shi, arXiv:1604.02116 .
- [75] K. Deng, G. Wan, P. Deng, K. Zhang, S. Ding, E. Wang, M. Yan, H. Huang, H. Zhang, Z. Xu, J. Denlinger, A. Fedorov, H. Yang, W. Duan, H. Yao, Y. Wu, y. S. Fan, H. Zhang, X. Chen, and S. Zhou, arXiv:1603.08508 .
- [76] A. Liang, J. Huang, S. Nie, Y. Ding, Q. Gao, C. Hu, S. He, Y. Zhang, C. Wang, B. Shen, J. Liu, P. Ai, X. Sun, W. Zhao, S. Lv, D. Liu, C. Li, Y. Zhang, Y. Hu, Y. Xu, L. Zhao, G. Liu, Z. Mao, X. Jia, S. Zhang, F. Yang, Z. Wang, Q. Peng, X. Dai, Z. Fang, Z. Xu, C. Chen, X. J. Zhou, E. Physics, and N. Orleans, arXiv:1604.01706 .
- [77] M. N. Ali, J. Xiong, S. Flynn, J. Tao, Q. D. Gibson, L. M. Schoop, T. Liang, N. Haldolaarachchige, M. Hirschberger, N. P. Ong, and R. J. Cava, *Nature* **514**, 205 (2014).
- [78] A. A. Soluyanov, D. Gresch, Z. Wang, Q. Wu, M. Troyer, X. Dai, and B. A. Bernevig, *Nature* **527**, 495 (2015).
- [79] Y. Wu, N. H. Jo, D. Mou, L. Huang, S. L. Bud'ko, P. C. Canfield, and A. Kaminski, arXiv:1604.05176 .
- [80] Y. Xu, F. Zhang, and C. Zhang, *Phys. Rev. Lett.* **115**, 265304 (2015).
- [81] Z. Yu, Y. Yao, and S. A. Yang, arXiv:1604.04030 .
- [82] G. E. Volovik, arXiv:1604.00849 .
- [83] M. Udagawa and E. J. Bergholtz, arXiv:1604.08457 .
- [84] A. A. Zyuzin and R. P. Tiwari, arXiv:1601.00890 .
- [85] L. Levitov, Y. Nazarov, and G. Eliashberg, *Zh. Eksp. Teor. Fiz.* **88**, 229 (1985).
- [86] V. Edelstein, *Solid State Commun.* **73**, 233 (1990).
- [87] S. Fujimoto and S. K. Yip, Chapter 8 in *Non-centrosymmetric Superconductors*, edited by E. B. Sigrist and M. (Springer-Verlag, Berlin, 2012).
- [88] V. M. Edelstein, *Sov. Phys. JETP* **68**, 1244 (1989).
- [89] V. M. Edelstein, *Phys. Rev. Lett.* **75**, 2004 (1995).
- [90] S. K. Yip, *Phys. Rev. B* **65**, 144508 (2002).
- [91] S. K. Yip, *J. Low Temp. Phys.* **140**, 67 (2005).
- [92] S. Fujimoto, *Phys. Rev. B* **72**, 024515 (2005).
- [93] V. M. Edelstein, *Phys. Rev. B* **72**, 172501 (2005).
- [94] S. Fujimoto, *J. Phys. Soc. Japan* **76**, 034712 (2007).
- [95] K. Maki, *Prog. Theor. Phys.* **29**, 10 (1963).
- [96] O. A. Tretiakov, D. Clarke, G. W. Chern, Y. B. Bazaliy, and O. Tchernyshyov, *Phys. Rev. Lett.* **100**, 127204 (2008).
- [97] K. Everschor, M. Garst, B. Binz, F. Jonietz, S. Mühlbauer,

- C. Pfleiderer, and A. Rosch, Phys. Rev. B **86**, 054432 (2012).
- [98] T. Schulz, R. Ritz, A. Bauer, M. Halder, M. Wagner, C. Franz, C. Pfleiderer, K. Everschor, M. Garst, and A. Rosch, Nat. Phys. **8**, 301 (2012).
- [99] R. Combescot and T. Dombre, Phys. Rev. B **33**, 79 (1986).
- [100] G. Volovik, Phys. B Condens. Matter **255**, 86 (1998).
- [101] T. D. C. Bevan, A. J. Manninen, J. B. Cook, J. R. Hook, H. E. Hall, T. Vachaspati, and G. E. Volovik, Nature **386**, 689 (1997).
- [102] C_2 rotational symmetry in point group T prohibits the off-diagonal components, and C_3 rotational symmetry makes the diagonal components the same in $K_{\mu\nu}$.
- [103] This is distinguished from the Magnus force, which does not require the excitation of quasiparticles.